Published in final edited form as:
Cancer Res. 2008 December 15; 68(24): 10145–10153. doi:10.1158/0008-5472.CAN-08-2992.

Wnt1 expression induces short- and long-range cell recruitments that modify mammary tumor development, and are not induced by a cell-autonomous β-catenin effector

Young Chul Kim[1], **Rod J. Clark**[1], **Erik A. Ranheim**[2], and **Caroline M. Alexander**[1,*]

[1] McArdle Laboratory for Cancer Research, University of Wisconsin-Madison

[2] Clinical Health Sciences, School of Medicine and Public Health, University of Wisconsin-Madison

Abstract

Xenograft model studies have shown that tumor associated, or genetically modified, activated stromal cells can promote tumor cell growth. Here, we examined mammary tumors arising in response to two different transgene-mediated Wnt signaling effectors: Wnt1 (a ligand with cell non-autonomous effects) and ΔNβ-catenin (a constitutively active form of the intracellular effector). Though the route of tumor development has been shown to be similar for these two models, histological analysis shows that Wnt1-induced tumors are associated with tracts of activated stroma, whereas most ΔNβ-catenin-induced tumors are solid adenocarcinomas. Furthermore, quantification of the "reactive stroma index" indicates that abundant activated stroma correlates with accelerated tumor progression. Wnt1-expressing mammary epithelial cells induce Wnt-specific target gene expression in local stromal cells (WISP1/CCN4), but also induce long-range effects. Thus, mice with rapid tumor progression have 2 fold more circulating endothelial progenitor cells in peripheral blood than control or ΔNβ-catenin transgenic mice. Using tagged bone marrow (BM) transplants, we show that BM-derived cells are massively recruited to infiltrate the stroma of Wnt1-induced tumors where they differentiate into multiple cell types. Thus, localized ectopic expression of the proto-oncogene Wnt1 in mammary glands induces systemic responses, and we propose that this response modifies the tumorigenic outcome.

Keywords

Stroma; Wnt; Mammary tumor; Bone marrow-derived cells; Endothelial progenitor cells

Introduction

It has become clear that the interactions that occur between epithelial and stromal cells to regulate organ development and function are re-activated and exploited during tumor initiation and progression to produce unregulated growth and vascularization (1). Co-culture and *in vivo* grafting analyses show that the altered stromal cells (often referred to as "activated" or "reactive" stroma) promote tumorigenesis of non-tumorigenic epithelial cells (2–4). Recent studies also suggest that stromal cells undergo genetic or epigenetic alteration as they respond to tumor cells (5–7), and that genetically modified stromal cells can initiate tumor development of epithelial cells (8). Stromal changes are known to occur in breast tumors. For instance, infiltrating ductal carcinomas, the most common type of breast cancer, show remarkable changes of stromal cell gene expression profile, extracellular matrix composition, and stromal

*Correspondence: CM Alexander alexander@oncology.wisc.edu.

cell morphology (9,10). Specific changes have recently been implicated as a functional component of tumor progression by their consistent association with tumors with poor prognosis (11,12). Since stroma comprises many organ-specific cell types, the elucidation of functional interactions requires the observation of the whole tumor process *in situ*, followed by deconstruction *in vitro*.

Wnt family members mediate epithelial-mesenchymal interactions during a variety of organogenic processes, including tooth, kidney, and mammary gland (13–15). Although Wnt ligands can induce several different signaling cascades, only the stabilization of β-catenin and binding to TCF/LEF transcription factor family members (the "canonical" pathway) has been shown to be tumorigenic, and aberrant activation of canonical Wnt signaling is implicated in a variety of human tumors (16,17). Wnt transactivational responses are highly cell type-specific and have been characterized for mammary gland (18). However, the genes that are key to the mammary oncogenic program are not yet known.

Transgenic mice ectopically expressing Wnt1 ligand or a constitutively active form of β-catenin (ΔNβ-catenin) in mammary glands under the control of an MMTV-LTR promoter develop mammary tumors (19,20). The origin of both Wnt1- and ΔNβ-catenin-induced adenocarcinomas appears to be similar. Both effectors induce the accumulation of stem/progenitor cells, and both induce highly differentiated (and bilineal) adenocarcinomas in a hyperplastic background (21,22). Here, we show that only Wnt1-induced preneoplastic hyperplasias and tumors are associated with activated stroma. This resembles the fibrotic stroma induced by ectopic overexpression of matrix metalloprotease-3 (23,24). We propose that Wnt1 expression in mammary epithelial cells activates neighboring stromal cells by a paracrine mechanism, while ΔNβ-catenin is a cell-autonomous effector. By comparing the mechanism of tumor development in these two transgenic strains, the physiological consequences of stromal activation can be evaluated *in vivo*. We show that abundant activated stroma correlates with more aggressive tumor development, and it is accompanied by the infiltration of bone marrow derived cells that contribute to angiogenesis and stromalization.

Materials and Methods

Mice

All mice used in this study were FVB/NJ background. *MMTV-Wnt1* mice were purchased from the Jackson Lab, and *MMTV-ΔNβ-catenin* mice were made and described by Dr. Pam Cowin (20). *Rosa26-hPAP* mice were kindly provided by Dr. Eric Sandgren (University of Wisconsin). The transgenic lines were bred through male hemizygotes. To determine the onset of mammary tumor formation, mice were palpated weekly (sensitive to 1 mm tumor masses).

Reactive stroma index

A representative H&E-stained section per tumor was examined by five blinded observers and scored for the reactive stroma index based on % contribution of stroma area in tumor mass (i.e., 0–10% stroma area=0, 11–20% stroma area=1, and so on, >50% stroma area=5). The average of five points was used as the reactive stroma index for each sample.

Antibody biotinylation

Mouse monoclonal anti-hPAP antibody (clone 8B6, Sigma) and a polyclonal anti-WISP1 antibody (sheep polyclonal, R&D Systems, MN) were biotinylated with a protein biotinylation kit (Dojindo Molecular Tech.) as instructed by the manufacturer.

Immunohistochemistry

We used standard methods to assay protein expression by immunohistochemistry. Antibodies used in this study are as follows: anti-K5 (1:300, rabbit polyclonal, Covance), anti-FSP1 (1:100, rabbit polyclonal, Dako), anti- CD31 (clone MEC7.46, 1:50, Abcam), anti-von Willebrand factor (1:200, rabbit polyclonal, Dako), anti-FITC conjugated α-SMA (clone 1A4, 1:250, Sigma), anti-F4/80 (clone CI:A3-1, 1:100, AbD Serotec), Cy3 conjugated donkey anti-rat IgG (1:100, Jackson ImmunoResearch), Alexa Fluor 546-goat anti-rabbit IgG (1:250, Molecular Probes), Alexa Fluor 488-goat antirabbit IgG (1:200, Molecular Probes).

Preparation of NMFs/HAFs and growth curve determination

To generate immortalized normal mammary fibroblast cells (NMFs) or Wnt1-induced hyperplasia-associated fibroblast cells (HAFs), mammary fat pad from adult FVB control or FVB-*MMTV-wnt1* mice were chopped with scissors into ~1 mm^3 chunks, and then digested with collagenase (3 mg/ml; Worthington) and trypsin (1.5 mg/ml; Worthington) for 90 min at 37°C with agitation. Enzyme digested tissues were washed with medium, and then filtered through a 40 μm cell strainer. The filter-through fraction was mostly single cells and small organoids, and these were plated on tissue culture plates. After a one-hour incubation at 37°C, unattached cells (mostly organoids and epithelial cells) were washed off using PBS. Only fibroblast cells grew out in DMEM+10% FBS medium, deduced from their expression of the fibroblast markers (FSP1 and SMA), and their lack of epithelia marker expression (K8 and K5) (data not shown).

To determine growth rate, 2×10^4 cells were plated per well of 24-well plates in 10% FBS +DMEM medium. After overnight incubation, medium was changed to either fresh 10% or 2% FBS containing medium. Total cell number was determined by trypsinization followed by counting using hematocytometer. Growth curve was plotted using average number of triplicate and standard deviation.

Quantification of microvessel density and tumor associated macrophage (TAM) density

CD31 or F4/80 stained tissue images were processed with ImageJ software to determine the total area of marker-positive cells ($pixel^2$). For comparison of samples, the area determination was divided by the total number of nuclei in the field, using ImageJ plug-in software, ITCN (Center for Bio-Image Informatics at UC-Santa Barbara). The procedure for image processing is described in detail in the supplemental files.

FACS

To quantify circulating endothelial progenitor cell number, peripheral blood (PB) cells were collected in PBS with 50 mM EDTA after heart puncture, and incubated in ALK buffer (150 mM NH_4Cl, 10 mM $KHCO_3$, 0.1 mM EDTA, pH 7.3) on ice for 10 min to lyse red blood cells. Cells were washed two times with HBS (Hank's balanced saline)+2% FBS (HF), and cell number was counted using a hemocytometer to calculate the total PB cell number per 1 ml of blood. Cells were resuspended in incubation buffer (2% FBS, 20 mM HEPES, 2 mM EDTA in DMEM), and then labeled with anti-CD45-FITC (clone 30-F11, eBioscience), anti-CD34-APC (clone RAM34, eBioscience), and anti-Flk1-PE (clone Avas 12α1, BD Biosciences) antibodies at 4°C for 30 min. After washing twice with cold HF, cells were resuspended in HF containing propidium iodide (PI, 5 μg/ml) and sorted using FACS Caliber (BD Biosciences). PI-negative live cells were gated and analyzed for their expression of $CD45^{low}CD34^{+}Flk1^{+}$ (characterizing the EPC population) using Flowjo (Treestar Inc.) software. The absolute number of EPCs was calculated by multiplying the % EPCs (typically less than 0.015%) by the total number of PB cells per ml of blood, as described by Asahara et al. (25).

Bone marrow transplant

5~7 week old female transgenic mice were irradiated with 4.5 Gray γ irradiation twice, separated by 3 hours. 10^6 whole bone marrow cells from FVB-*Rosa26-hPAP* mice were injected retroorbitally. Reconstitution of the hematopoietic lineage was confirmed by assaying the expression of heat-resistant alkaline phosphatase on the cell surface of peripheral blood cells 4 weeks after transplantation. The % reconstitution was > 99%. Mice were sacrificed when tumors were palpable, and tumors were removed and either fixed in 4% PFA in PBS for overnight or embedded in OCT solution for immunohistochemical analysis.

Tumor cell dissociation and isograft

Tumor cells were isolated as described by Orimo et al. (25) with some modifications. Briefly, chopped tumors were incubated in the dissociation buffer (1 g tissue/4 ml buffer; 1 mg/ml collagenase type I (Boehringer Mannheim), 125 units/ml hyaluronidase (Sigma), 20 mM Hepes buffer (pH 7.5), 10% FBS in DMEM) for 3 hrs at 37°C with agitation. Fresh cold medium (10% FBS+DMEM) was added to enzyme digested cells, and then centrifuged at 400 g for 10 min. Cells were resuspended with medium, and single cells were prepared by filtering through a 40 μm cell strainer. Red blood cells were lysed by incubating them in ALK buffer (150 mM NH_4Cl, 10 mM $KHCO_3$, 0.1 mM EDTA, pH 7.3).

For isografts of tumor cells, isogenic 3 week-old FVB female mice were anesthetized using avertin, and endogenous epithelia of inguinal mammary fat pads were surgically removed. 5×10^3 tumor cells were counted and suspended in DMEM+2% FBS with 5 μg/ml Matrigel (BD Biosciences) and injected into a small pocket that was made using a surgical forceps in the fad pad as described previously (22).

Statistical analysis

All data sets were compared by two-sided Wilcoxon rank sum test using Mstat software (Dr. Norman Drinkwater, University of Wisconsin). All data were presented as means with standard deviation error bars.

Real-time quantitative PCR (qPCR)

Inguinal #4 mammary glands were dissected out and lymph nodes were surgically removed, and then tissues were stored in RNAlater solution (Ambion, TX). Total RNA was isolated using RNeasy Lipid Tissue Mini Kit (Qiagen, CA) as instructed by the manufacturer. 750 μg of total RNA was reverse transcribed in 60 μl reaction volume using QuantiTect Rev. Trasnscription Kit (Qiagen, CA). 1 μl of cDNA was mixed with 5 μl of Platinum Super Mix (Platinum SYBER Green qPCR SuperMix-UDG with Rox, Invitrogen) and 4 μl of forward and reverse primer (0.5 μM), and the PCR was performed using ABI7900-HT (50°C-2 min, 95°C-2 min, 45 cycles of 95°C-15 sec; 53°C-30 sec; 72°C-30 sec, and followed by a dissociation curve). Further details of the normalization procedure and primer sequences are provided in the Supplementary file.

Results

Wnt1-induced hyperplasias and tumors are associated with activated stroma

Wnt signaling is required for embryonic mammary placode formation and is at least partly mediated by peri-epithelial stroma (15). Several Wnt ligands are expressed during embryonic and juvenile mammary development, though not Wnt1 (26).

In order to determine whether activated stroma is present in Wnt1-expressing mammary tissues, we compared the histological features of tissues from *MMTV-Wnt1* mice with tissues

from *MMTV-ΔNβ-catenin* mice and non-transgenic control mice. Since activated stroma is often associated with collagen deposition (9), we analyzed mammary tissue sections from 3 month old animals that were stained with Masson's Trichrome (Fig. 1A). Both Wnt1- and ΔNβ-catenin-expressing mammary glands developed preneoplastic hyperplasia at this age, but only Wnt1-expressing hyperplastic glands were extensively surrounded by collagen-rich (blue-stain) matrix with embedded stromal cells.

Differences with respect to stromal activation were even more evident for Wnt1-induced tumors. Histological examination of H&E-stained tumor sections showed that most Wnt1-induced tumors were associated with tracts of activated stroma, whereas most ΔNβ-catenin induced tumors were solid adenocarcinomas which were encapsulated with a stromal sheath, but showed little infiltration (Fig. 1B, top panel). In order to assess whether tumor-associated stromal cells display reactive stroma markers, tumor sections were stained with myofibroblast cell marker, α-smooth muscle actin (SMA) (27). Since SMA is also expressed in myoepithelial cells, tumor sections were co-stained with a myoepithelial cell marker, K5, to distinguish two different cell types. Thus, immunohistochemical analyses showed that the stromal tracts were indeed enriched in SMA-positive fibroblasts (Fig. 1B, bottom panel), and in many cases, those activated stromal cells also expressed another activated fibroblast cell marker, FSP1 (data not shown).

These histological features were also found in *MMTV-Wnt1* mice crossed to a *C57/Bl6* background (data not shown) and were evident in tumors from independently generated strains of transgenic Wnt1 and mutant β-catenin mice (28,29). Furthermore, Wnt10b-induced tumors displayed a fibrotic stroma that was histologically similar to Wnt1-induced tumors (30). Therefore, this is a robust phenotype that associates with the expression of epithelial Wnt ligands.

Abundant stroma correlates with accelerated tumor progression

Both Wnt1 and ΔNβ-catenin induced tumor formation with quite high penetrance (77% and 96%, respectively) in a year time period, but with quite different kinetics (Fig. 1C). Tumor onset (defined as the time for 10% of mice to develop tumors) was much more rapid in *MMTV-Wnt1* mice (6.3 weeks, n=48), compared to 18 weeks in *MMTV-ΔNβ-catenin* mice (n=25, Supplemental Table 1). Indeed, 40% of *MMTV-Wnt1* mice developed tumors prior to 120 days of age, compared to less than 10% *MMTV-ΔNβ-catenin* mice. In contrast, the rest of *MMTV-Wnt1* mice that did not develop tumors rapidly appeared to be relatively tumor-resistant, so tumors appeared slowly or not at all (reflected in the penetrance). Accordingly, *MMTV-Wnt1* mice appear to fall into (at least) two groups; one with aggressive tumor progression, and the other with delayed or not tumor progression.

In order to quantify the grade of stromal activation for early and late developing Wnt1- induced tumors, we classified Wnt1-induced tumors into two groups (Group 1, tumors that developed prior to 120 days of age (n=19) and Group 2, tumors (n=15) that developed later than 120 days). The stromal indices were measured in a blinded fashion as described in Materials and Methods. Group 1 Wnt1-induced tumors have 30% higher reactive stroma indices than Group 2 tumors (3.9 ± 0.8 compared to 3.0 ± 1.1 respectively; P=0.026), correlating abundant stroma with accelerated tumor progression. Interestingly, 60% of Group 2 Wnt1-induced tumors displayed hemorrhagic "blood lakes" (Supplemental files; Fig. 1), whereas this was uncommon in Group 1 Wnt1-induced tumors (16%). This may indicate more leaky tumor vascular structures, or higher rates of necrosis in Group 2 Wnt1-induced tumors.

ΔNβ-catenin-induced tumors were also (arbitrarily) divided into two approximately equal-sized groups for comparison with the Wnt1 transgenic cohort (Group 1, n=7, less than 190 days and Group 2, n=8, 190–360 days). None of these tumors were significantly associated

with stromal cells (Group 1=1.6 ± 1.0; Group 2= 1.2 ± 1.2), and there was no significant difference between Group 1 and Group 2 tumors.

Previous studies suggest that the MMTV-LTR is also active in several hematopoietic cell types (31). Therefore, we assessed whether the recruitment of BM-derived cells in Wnt1-induced tumors was an artifact of ectopic MMTV-driven Wnt1 expression in hematopoietic cells, by isografting tumor cells into non-transgenic hosts. Wnt1 and ΔNβ-catenin tumor cells were prepared, and 5×10^3 tumor cells were transplanted into cleared fat pads of 3 week-old control female mice. Both Wnt1 and ΔNβ-catenin isografts formed palpable tumors in 45 days. Importantly, they formed histologically identical tumors to the typical Wnt1- or ΔNβ-catenin-induced tumors (Fig. 1D). Thus, tumors from Wnt1 tumor cell isografts are associated with activated stromal tracts and blood lakes whereas tumors from ΔNβ-catenin tumor cell isografts form solid adenocarcinomas. Furthermore, transplantation of Wnt1 tumors cells to β-actin-GFP transgenic hosts induced recruitment of GFP^+ host cells and BM-derived cells during tumor formation (B. Liu and P. Polakis, personal communication). Accordingly, we propose that expression of Wnt1 in hematopoietic cells is not required for inducing short- and long-range recruitment. Rather, Wnt1 expressing tumor cells are sufficient to activate surrounding stromal cells and recruit BM-derived cells.

Wnt1 activates surrounding stromal cells

Wnt proteins are lipid modified and often considered to be short-range morphogens, or even to act as autocrine factors, depending upon the extracellular milieu (32,33). For example, the short cellular range of Wnt signaling has been specifically visualized during limb development, using an *Axin2* reporter gene, and found to be a few cells deep (D. T. Berge and R. Nusse, unpublished). Since *MMTV-Wnt1* is expressed in luminal cells (31) and therefore separated from stromal cells by the myoepithelium and basement membrane, it is important to determine whether Wnt1 directly activates surrounding stromal cells or recruits them by an indirect mechanism. Previous studies from other groups have shown that *WISP*1 (Wnt1 induced secreted protein 1; CCN4) is a Wnt1/β-catenin target gene expressed specifically in the fibroblasts surrounding Wnt1-expressing tumor cells (34,35). Accordingly, we assessed the induction of *WISP1* mRNA expression in transgenic mammary glands by real time quantitative PCR (qPCR) assay. Interestingly, *WISP1* expression was induced ~ 5 fold in Wnt1-expressing mammary glands, but not in ΔNβ-catenin-expressing glands (or controls; Fig. 2A). In order to determine whether ectopic ΔNβ-catenin expression induces canonical Wnt signaling, the expression level of Wnt/β-catenin target gene, *Axin2* (36) was also evaluated using the same total RNA samples (Fig. 2B). *Axin2* has been shown to be a uniquely robust and universal Wnt/β-catenin target gene (18,37,38). Wnt1-expressing glands have 1.7 fold more *Axin2* mRNA than control mammary glands ($P<0.001$). On the other hand, ΔNβ-catenin-expressing glands have 4 fold more *Axin2* mRNA levels compared to control, and 2.3 fold more than Wnt1 expressing glands ($P<0.01$), indicating that ΔNβ-catenin expression activates canonical Wnt signaling in mammary gland and it is a more potent canonical signaling agonist than Wnt1. Furthermore, we also confirmed that WISP1 protein was associated with the stroma of Wnt1-induced tumors (Fig. 2C), which is consistent with previously reported results of *in situ* hybridization of mRNA (34). Therefore, we propose that Wnt1 directly activates signaling in nearby stromal cells by a paracrine mechanism.

To determine whether ectopic Wnt1 expression affects the growth potential of surrounding stromal cells, we prepared stromal cells from control mammary glands (referred to as normal mammary fibroblasts or NMFs) or Wnt1-induced hyperplastic mammary glands (referred to as hyperplasia-associated fibroblasts or HAFs) and compared their growth rates (Fig. 2D). In high serum (10% FBS) media, HAFs grew much faster compared to NMFs. Whereas NMFs arrested in low serum (2% FBS), HAFs survived and divided, indicating that HAFs have

persistent changes of their phenotype, that are maintained in tissue culture condition. To test the effect of Wnt treatment on fibroblasts, NMFs were incubated in Wnt3a conditioned media or control media (contains <2% FBS) and were found to survive over 10 days of culture with added Wnt3a, but not without (Supplemental files; Fig. 2). Taken together, these data suggest that Wnt ligands are survival/growth factors for mammary fibroblast cells, and that the stromal fibroblast components of Wnt1-induced hyperplasia may have acquired genetic or epigenetic alterations that result in increased growth/survival potential.

Angiogenesis in Wnt1-induced tumors

Because angiogenesis is a rate-limiting step in tumor progression and has been proposed to be recruited by reactive stroma (39), we compared tumor vascularization for Group 1 Wnt1- and ΔNβ-catenin-induced tumors. Tumor sections were stained with anti-CD31 antibody to quantify microvessel density (determined by CD31-positive area (pixel^2) per cell; Fig. 3A and Supplemental files; Fig. 3). Analysis of 72 fields (5~8 different fields per tumor, for each of 6 Wnt1-induced tumors, and 5 ΔNβ-catenin-induced tumors) showed no significant difference between Wnt1- and ΔNβ-catenin-induced tumors in microvessel density (Fig. 3A, bottom left panel). However, we found that ~55% of microvessels in Wnt1-induced tumors were associated with activated stromal tracts (Fig. 3A, bottom right panel), while vessels in ΔNβ-catenin-induced tumors were mostly mixed with tumor cells, some of which had a dilated structure (*, Fig. 3A). Further high-resolution analysis showed that vessels embedded in the activated stroma (SMA$^+$ myofibroblast cells rich area) had a relatively thin and serpentine structure (arrow, Fig. 3B) whereas tumor cell-associated vessels were most often aggregates of CD31$^+$ endothelial cells (arrow head, Fig. 3B) that resemble the dilated vessels in ΔNβ-catenin induced tumors (Fig. 3B). Taken together, these data suggested that we should test whether there were differences between the angiogenic mechanisms that supported these two tumor types.

Abundant stroma correlates with higher numbers of circulating EPCs

Accumulating evidence suggests that bone marrow (BM)-derived endothelial progenitor cells (EPCs) play a role in the angiogenesis that accompanies pathogenic changes, including tumorigenesis (40). Additionally, studies have shown that carcinoma-associated fibroblasts promote tumor angiogenesis by mobilizing and recruiting EPCs (25). Therefore, we assessed whether Wnt1-activated stroma induces the mobilization of EPCs. To quantify EPC mobilization, the EPC-enriched population (CD45^{low}CD34$^+$Flk1 (VEGFR2)$^+$ cells) was quantified in peripheral blood cells from control (age-matched non-transgenic littermates), Wnt1-, and ΔNβ-catenin-induced tumor-bearing mice by flow cytometry (41) (Fig. 4). Group 1 Wnt1-induced tumor-bearing mice had over 2 fold more circulating EPCs compared to control and Group 2 Wnt1-induced tumor-bearing mice ($P<0.02$). Although the difference was not statistically significant ($P=0.062$), Group 1 Wnt1-induced tumor-bearing mice had ~1.8 fold more circulating EPCs than ΔNβ-catenin-induced tumor-bearing mice. Therefore, these data suggest that abundant activated stroma and accelerated tumor development correlate with higher numbers of circulating EPCs.

BM-derived cells are recruited to Wnt1-induced tumors

In order to examine the contribution of BM-derived cells to tumor vascularization, we transplanted BM cells from *Rosa26-hPAP* (human placenta alkaline phosphatase) mice into lethally irradiated *MMTV-Wnt1* and *MMTV-ΔNβ-catenin* mice (Fig. 5). These irradiated transgenic mice developed tumors with similar kinetics and pathological phenotypes to the nonirradiated transgenic mice (data not shown). Tumors from chimeric bone marrow transgenic mice were removed and examined by immunohistochemistry using biotin-conjugated hPAP antibody. BM-derived cells (hPAP$^+$) were extensively recruited to Wnt1-

induced tumors, while only a few hPAP$^+$ cells were present in ΔNβ-catenin-induced tumors (Fig. 5A).

To determine whether BM-derived cells incorporated into newly formed blood vessels, tumor sections were co-stained with biotin-hPAP and either CD31 or von Willebrand factor antibodies (Fig. 5B). Interestingly, most hPAP$^+$ cells were perivascular, and only a subpopulation of endothelial cells was hPAP and CD31 or von Willebrand factor double positive (arrow). The quantitative analysis (total 64 different fields; 8 fields/tumor, described as % double positive cells/total endothelial cells) showed that there were ~2 fold more vessel-incorporated BM-derived cells in Wnt1-induced tumors than ΔNβ-catenin-induced tumors (P=0.02), which parallels the number of circulating EPCs (Fig. 5C). BM-derived cells were enriched in stroma-associated vessels compared to epithelial tumor cells.

We assessed the tumor-associated fibroblast cells that were derived from BM (42). Double-labeling with biotin-hPAP and FSP1 antibodies showed that a high proportion of FSP1$^+$ cells in the infiltrated stromal area of Wnt1-induced tumors were hPAP$^+$ BM-derived cells whereas only a few FSP1+ cells were present in ΔNβ-catenin-induced tumors (arrow, Fig. 5D). Thus, Wnt1-expressing tumor cells induce infiltration of BM-derived cells that contribute to tumor vascularization and stromalization.

More tumor-associated macrophages are recruited to Wnt1-induced tumors

Tumor-associated macrophages (TAMs) have been shown to modify breast tumor development and metastasis (43). To evaluate whether stromal recruitment was associated with the recuitment of TAMs, we quantified the number of F4/80 (pan-macrophage marker)-positive cells in Wnt1- and ΔNβ-catenin-induced tumors (Fig. 6). Wnt1-induced tumors showed a ~2.5 fold increase F4/80-positive area per cell compared to ΔNβ-catenin-induced tumors (Fig. 6A). The majority of TAMs in Wnt1-induced tumors were associated with stromal tracts, whereas TAM in ΔNβ-catenin-induced tumors mostly resided in the lumen of blood vessels (Fig. 6B).

Discussion

Our data show that localized production of Wnt1 ligand in the mammary gland is associated with a systemic response, including localized stromal activation, long-range (humoral) bone marrow activation, endothelial precursor cell mobilization, and the infiltration of macrophages. Though the Wnt signaling pathway is necessary for normal morphogenesis (including mammary development (44)), dysregulation is highly oncogenic for (many) epithelia. Though Wnt ligands stimulate several signaling pathways, only the β-catenin/TCF canonical route has been shown to be oncogenic. We compared the process of breast tumor development in response to a secreted Wnt1 ligand with that observed in response to the cell-autonomous ΔNβ-catenin Wnt effector, and found that the disease process was much more complex when Wnt ligands were ectopically expressed. Thus, some tumors appeared much faster, whereas other mice were delayed or prevented from developing tumors. ΔNβ-catenin-induced tumors are less morphologically heterogeneous, contain minimal stroma and are more uniform in their time of appearance (median latency). Since the tumor precursor cell and the oncogenic signaling pathway are presumed to be similar for both models, we propose that the variability of the final tumor load in the Wnt1 strain derives from altered tumor progression mediated by the stroma and subsequent body response.

Activation of stromal cells by Wnt signaling pathways

We have shown that stromal activation (measured as enlarged stromal compartments, expression of desmoplastic markers such as SMA, and activation of Wnt target genes such as *WISP1*) is a feature of preneoplastic Wnt1-expressing glands, but not β-catenin-induced glands.

Therefore, stromal activation must depend directly upon Wnt1 ligand signaling, and not upon a molecule induced by epithelial cell β-catenin/TCF transactivation.

We propose that a non-canonical Wnt response is involved in stromal activation. Thus, although canonical Wnt signaling (via a Frizzled-LRP pair) clearly induces the accumulation of nuclear ΔNβ-catenin in cultured fibroblasts, we could not observe a similar phenomenon *in vivo* in these glands (data not shown). However, we have shown that Wnt1 expression in mammary epithelial cells induces the Wnt target gene, *WISP1*, in the subjacent stroma (Fig. 2A & C). Data from another group suggests that although there are TCF-binding sites in the WISP1 promoter, it is the CREB binding site that directs transactivation in response to Wnt1 or ΔNβ-catenin (35). This is confirmed by a recent report that ascribes the physiological effects of noncanonical Wnt signaling to ATF/CREB-mediated transactivation (45). These effects are likely mediated by Frizzled alone, or by alternate Wnt receptors (such as Ror). During development, these non-canonical pathways are key to morphogenetic movements of whole embryos, and to cell motility.

Wnt1-expressing mammary epithelial cells can recruit BM-derived cells during tumor development

Our present study shows that Wnt1 expressing-tumor cells can mobilize EPCs and recruit BM-derived cells. Thus, we find that the pattern of stromal colonization in isografts is characteristic of the primary tumor. When aggressive tumors, with high stromal colonization, are isografted to virgin mammary fat pads, their phenotype is similar (Fig. 1D). It is therefore unlikely that there is a stochastic host-derived switch that determines the tumor-stromal phenotype. These BM-derived cells then differentiate into various cell types including endothelial cells and fibroblast cells. Furthermore, Wnt1-induced tumors are associated with ~2.5 fold more macrophages than ΔNβ-catenin-induced tumors. These observations indicate that Wnt1 expressing-tumor cells are capable of communicating with circulating or resting BM cells and recruiting them to the tumor site. Wnt proteins are lipid modified and interact with heparan sulfates, and are usually considered short-range morphogens (32,33). However, reports suggest there may be lipid carriers that could turn Wnt ligands into humoral agents (46). Our preliminary experiments could not find blood-borne Wnt signaling activity in serum from Wnt transgenic mice (using a very sensitive reporter assay *in vitro*; data not shown).

We propose instead that mammary stroma expresses a bioactive recruiting molecule in response to Wnt1 interaction. Two obvious candidates are SDF1 (stromal cell-derived factor 1) and VEGF (vascular endothelial growth factor). These have been shown to be major chemokines that mediate mobilization and recruitment of BM-derived cells. VEGF administration increases circulating EPCs *in vivo* (47), and ectopic expression of VEGF induces homing of circulating mononuclear myeloid cells (48). SDF1 expression is induced in hypoxic lesions, and it increases the migration and homing of circulating $CXCR4^+$ progenitor cells (49). In addition, tumor-associated fibroblast cells express higher level of SDF1, which correlates with more circulating EPCs (25). However, we could not find evidence in support of a role for either of these mediators. Instead, using qPCR analyses, we found that Wnt1-induced hyperplastic mammary glands and tumors have ~2 fold less *SDF1α* and *VEGFα* mRNA level compared to control mammary glands (data not shown). We have broadened the search for the paracrine effector that communicates to bone marrow.

Whereas there is little direct data to support a major role of canonical Wnt signaling during the initiation of human breast tumors, there is data that suggests that the loss of the extracellular Wnt pathway inhibitor, SFRP1 (Secreted Frizzled-related protein1), is important to breast cancer (50). Furthermore, a recent study showed that *FZDB*, a negative Wnt signaling regulator, is down-regulated in breast cancer-associated stroma compartment and that it correlates with poor prognostic outcome (11), suggesting the important role of stromal Wnt signaling

activation in breast cancer development. Given the widespread expression of “non-canonical” Wnt ligands in mammary gland, our data suggest that up-regulated extracellular Wnt signaling could represent a mechanism for inducing localized stromal activation, and systemic recognition of the pre-malignant lesion by the body.

Supplementary Material

Refer to Web version on PubMed Central for supplementary material.

Acknowledgments

We thank Andreas Friedl and Bob Liu for help during the preparation of this manuscript. This work was supported by the National Cancer Institute RO1 CA90877, and by the McArdle Lab Training Award (YCK) T32 CA09135.

Abbreviations

ΔNβ-catenin	β-catenin with deletion of the N-terminal 89 amino acids
MMTV-LTR	Mouse mammary tumor virus-long terminal repeat
FACS	Fluorescent-activated cell sorting

References

1. Bissell MJ, Radisky D. Putting tumours in context. Nat Rev Cancer 2001;1(1):46–54. [PubMed: 11900251]
2. Barcellos-Hoff MH, Ravani SA. Irradiated mammary gland stroma promotes the expression of tumorigenic potential by unirradiated epithelial cells. Cancer Res 2000;60(5):1254–60. [PubMed: 10728684]
3. Olumi AF, Grossfeld GD, Hayward SW, Carroll PR, Tlsty TD, Cunha GR. Carcinoma-associated fibroblasts direct tumor progression of initiated human prostatic epithelium. Cancer Res 1999;59(19): 5002–11. [PubMed: 10519415]
4. Skobe M, Fusenig NE. Tumorigenic conversion of immortal human keratinocytes through stromal cell activation. Proc Natl Acad Sci U S A 1998;95(3):1050–5. [PubMed: 9448283]
5. Kurose K, Gilley K, Matsumoto S, Watson PH, Zhou XP, Eng C. Frequent somatic mutations in PTEN and TP53 are mutually exclusive in the stroma of breast carcinomas. Nat Genet 2002;32(3):355–7. [PubMed: 12379854]
6. Hill R, Song Y, Cardiff RD, Van Dyke T. Selective evolution of stromal mesenchyme with p53 loss in response to epithelial tumorigenesis. Cell 2005;123(6):1001–11. [PubMed: 16360031]
7. Hu M, Yao J, Cai L, Bachman KE, van den Brule F, Velculescu V, et al. Distinct epigenetic changes in the stromal cells of breast cancers. Nat Genet 2005;37(8):899–905. [PubMed: 16007089]
8. Bhowmick NA, Chytil A, Plieth D, Gorska AE, Dumont N, Shappell S, et al. TGF-beta signaling in fibroblasts modulates the oncogenic potential of adjacent epithelia. Science 2004;303(5659):848–51. [PubMed: 14764882]
9. Ronnov-Jessen L, Petersen OW, Bissell MJ. Cellular changes involved in conversion of normal to malignant breast: importance of the stromal reaction. Physiol Rev 1996;76(1):69–125. [PubMed: 8592733]
10. Allinen M, Beroukhim R, Cai L, Brennan C, Lahti-Domenici J, Huang H, et al. Molecular characterization of the tumor microenvironment in breast cancer. Cancer Cell 2004;6(1):17–32. [PubMed: 15261139]
11. Finak G, Bertos N, Pepin F, Sadekova S, Souleimanova M, Zhao H, et al. Stromal gene expression predicts clinical outcome in breast cancer. Nat Med 2008;14(5):518–27. [PubMed: 18438415]
12. Finak G, Sadekova S, Pepin F, Hallett M, Meterissian S, Halwani F, et al. Gene expression signatures of morphologically normal breast tissue identify basal-like tumors. Breast Cancer Res 2006;8(5):R58. [PubMed: 17054791]

13. Vainio S, Muller U. Inductive tissue interactions, cell signaling, and the control of kidney organogenesis. Cell 1997;90(6):975–8. [PubMed: 9323125]

14. Kratochwil K, Galceran J, Tontsch S, Roth W, Grosschedl R. FGF4, a direct target of LEF1 and Wnt signaling, can rescue the arrest of tooth organogenesis in Lef1(−/−) mice. Genes Dev 2002;16(24): 3173–85. [PubMed: 12502739]

15. Boras-Granic K, Chang H, Grosschedl R, Hamel PA. Lef1 is required for the transition of Wnt signaling from mesenchymal to epithelial cells in the mouse embryonic mammary gland. Dev Biol 2006;295(1):219–31. [PubMed: 16678815]

16. Polakis P. Wnt signaling and cancer. Genes Dev 2000;14(15):1837–51. [PubMed: 10921899]

17. Logan CY, Nusse R. The Wnt signaling pathway in development and disease. Annu Rev Cell Dev Biol 2004;20:781–810. [PubMed: 15473860]

18. Clevers H. Wnt/beta-catenin signaling in development and disease. Cell 2006;127(3):469–80. [PubMed: 17081971]

19. Tsukamoto AS, Grosschedl R, Guzman RC, Parslow T, Varmus HE. Expression of the int-1 gene in transgenic mice is associated with mammary gland hyperplasia and adenocarcinomas in male and female mice. Cell 1988;55(4):619–25. [PubMed: 3180222]

20. Imbert A, Eelkema R, Jordan S, Feiner H, Cowin P. Delta N89 beta-catenin induces precocious development, differentiation, and neoplasia in mammary gland. J Cell Biol 2001;153(3):555–68. [PubMed: 11331306]

21. Li Y, Welm B, Podsypanina K, Huang S, Chamorro M, Zhang X, et al. Evidence that transgenes encoding components of the Wnt signaling pathway preferentially induce mammary cancers from progenitor cells. Proc Natl Acad Sci U S A 2003;100(26):15853–8. [PubMed: 14668450]

22. Liu BY, McDermott SP, Khwaja SS, Alexander CM. The transforming activity of Wnt effectors correlates with their ability to induce the accumulation of mammary progenitor cells. Proc Natl Acad Sci U S A 2004;101(12):4158–63. [PubMed: 15020770]

23. Sternlicht MD, Lochter A, Sympson CJ, Huey B, Rougier JP, Gray JW, et al. The stromal proteinase MMP3/stromelysin-1 promotes mammary carcinogenesis. Cell 1999;98(2):137–46. [PubMed: 10428026]

24. Wiseman BS, Werb Z. Stromal effects on mammary gland development and breast cancer. Science 2002;296(5570):1046–9. [PubMed: 12004111]

25. Orimo A, Gupta PB, Sgroi DC, Arenzana-Seisdedos F, Delaunay T, Naeem R, et al. Stromal fibroblasts present in invasive human breast carcinomas promote tumor growth and angiogenesis through elevated SDF-1/CXCL12 secretion. Cell 2005;121(3):335–48. [PubMed: 15882617]

26. Weber-Hall SJ, Phippard DJ, Niemeyer CC, Dale TC. Developmental and hormonal regulation of Wnt gene expression in the mouse mammary gland. Differentiation 1994;57(3):205–14. [PubMed: 7988795]

27. Sugimoto H, Mundel TM, Kieran MW, Kalluri R. Identification of fibroblast heterogeneity in the tumor microenvironment. Cancer Biol Ther 2006;5(12):1640–6. [PubMed: 17106243]

28. Michaelson JS, Leder P. beta-catenin is a downstream effector of Wnt-mediated tumorigenesis in the mammary gland. Oncogene 2001;20(37):5093–9. [PubMed: 11526497]

29. Gunther EJ, Moody SE, Belka GK, Hahn KT, Innocent N, Dugan KD, et al. Impact of p53 loss on reversal and recurrence of conditional Wnt-induced tumorigenesis. Genes Dev 2003;17(4):488–501. [PubMed: 12600942]

30. Lane TF, Leder P. Wnt-10b directs hypermorphic development and transformation in mammary glands of male and female mice. Oncogene 1997;15(18):2133–44. [PubMed: 9393971]

31. Wagner KU, McAllister K, Ward T, Davis B, Wiseman R, Hennighausen L. Spatial and temporal expression of the Cre gene under the control of the MMTV-LTR in different lines of transgenic mice. Transgenic Res 2001;10(6):545–53. [PubMed: 11817542]

32. Bradley RS, Brown AM. The proto-oncogene int-1 encodes a secreted protein associated with the extracellular matrix. Embo J 1990;9(5):1569–75. [PubMed: 2158444]

33. Coudreuse D, Korswagen HC. The making of Wnt: new insights into Wnt maturation, sorting and secretion. Development 2007;134(1):3–12. [PubMed: 17138665]

34. Pennica D, Swanson TA, Welsh JW, Roy MA, Lawrence DA, Lee J, et al. WISP genes are members of the connective tissue growth factor family that are up-regulated in wnt-1-transformed cells and

aberrantly expressed in human colon tumors. Proc Natl Acad Sci U S A 1998;95(25):14717–22. [PubMed: 9843955]

35. Xu L, Corcoran RB, Welsh JW, Pennica D, Levine AJ. WISP-1 is a Wnt-1- and beta-catenin-responsive oncogene. Genes Dev 2000;14(5):585–95. [PubMed: 10716946]
36. Jho EH, Zhang T, Domon C, Joo CK, Freund JN, Costantini F. Wnt/beta-catenin/Tcf signaling induces the transcription of Axin2, a negative regulator of the signaling pathway. Mol Cell Biol 2002;22(4): 1172–83. [PubMed: 11809808]
37. Huang S, Li Y, Chen Y, Podsypanina K, Chamorro M, Olshen AB, et al. Changes in gene expression during the development of mammary tumors in MMTV-Wnt-1 transgenic mice. Genome Biol 2005;6 (10):R84. [PubMed: 16207355]
38. Brack AS, Conboy MJ, Roy S, Lee M, Kuo CJ, Keller C, et al. Increased Wnt signaling during aging alters muscle stem cell fate and increases fibrosis. Science 2007;317(5839):807–10. [PubMed: 17690295]
39. Tuxhorn JA, Ayala GE, Rowley DR. Reactive stroma in prostate cancer progression. J Urol 2001;166 (6):2472–83. [PubMed: 11696814]
40. Rafii S, Lyden D, Benezra R, Hattori K, Heissig B. Vascular and haematopoietic stem cells: novel targets for anti-angiogenesis therapy? Nat Rev Cancer 2002;2(11):826–35. [PubMed: 12415253]
41. Bertolini F, Shaked Y, Mancuso P, Kerbel RS. The multifaceted circulating endothelial cell in cancer: towards marker and target identification. Nat Rev Cancer 2006;6(11):835–45. [PubMed: 17036040]
42. Direkze NC, Hodivala-Dilke K, Jeffery R, Hunt T, Poulsom R, Oukrif D, et al. Bone marrow contribution to tumor-associated myofibroblasts and fibroblasts. Cancer Res 2004;64(23):8492–5. [PubMed: 15574751]
43. Lewis CE, Pollard JW. Distinct role of macrophages in different tumor microenvironments. Cancer Res 2006;66(2):605–12. [PubMed: 16423985]
44. Lindvall C, Evans NC, Zylstra CR, Li Y, Alexander CM, Williams BO. The Wnt signaling receptor Lrp5 is required for mammary ductal stem cell activity and Wnt1-induced tumorigenesis. J Biol Chem 2006;281(46):35081–7. [PubMed: 16973609]
45. Zhou W, Lin L, Majumdar A, Li X, Zhang X, Liu W, et al. Modulation of morphogenesis by noncanonical Wnt signaling requires ATF/CREB family-mediated transcriptional activation of TGFbeta2. Nat Genet 2007;39(10):1225–34. [PubMed: 17767158]
46. Panakova D, Sprong H, Marois E, Thiele C, Eaton S. Lipoprotein particles are required for Hedgehog and Wingless signalling. Nature 2005;435(7038):58–65. [PubMed: 15875013]
47. Asahara T, Takahashi T, Masuda H, Kalka C, Chen D, Iwaguro H, et al. VEGF contributes to postnatal neovascularization by mobilizing bone marrow-derived endothelial progenitor cells. Embo J 1999;18 (14):3964–72. [PubMed: 10406801]
48. Grunewald M, Avraham I, Dor Y, Bachar-Lustig E, Itin A, Jung S, et al. VEGF-induced adult neovascularization: recruitment, retention, and role of accessory cells. Cell 2006;124(1):175–89. [PubMed: 16413490]
49. Ceradini DJ, Kulkarni AR, Callaghan MJ, Tepper OM, Bastidas N, Kleinman ME, et al. Progenitor cell trafficking is regulated by hypoxic gradients through HIF-1 induction of SDF-1. Nat Med 2004;10(8):858–64. [PubMed: 15235597]
50. Ugolini F, Charafe-Jauffret E, Bardou VJ, Geneix J, Adelaide J, Labat-Moleur F, et al. WNT pathway and mammary carcinogenesis: loss of expression of candidate tumor suppressor gene SFRP1 in most invasive carcinomas except of the medullary type. Oncogene 2001;20(41):5810–7. [PubMed: 11593386]

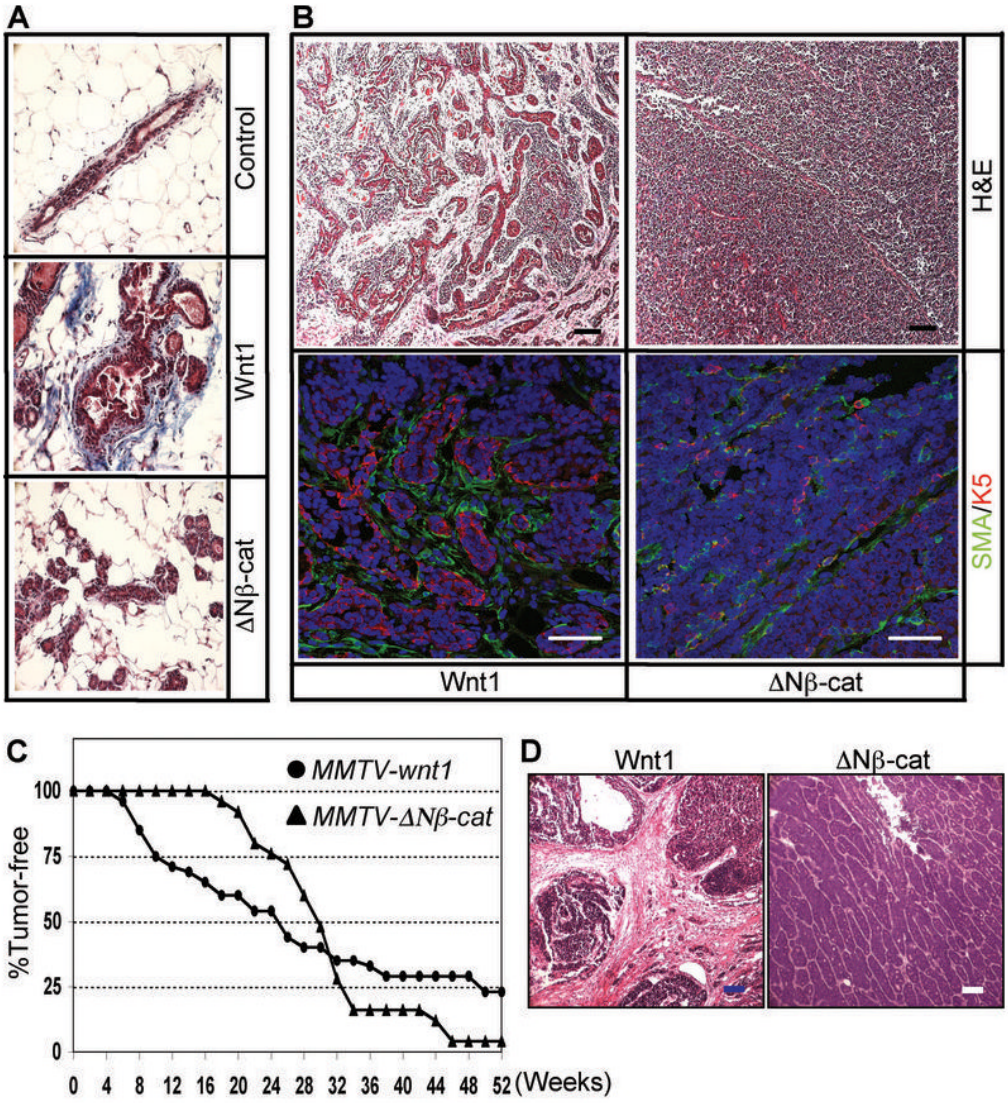

Figure 1.

Activated stroma in Wnt1-expressing preneoplastic hyperplastic glands and tumors. (A) Mammary tissue sections from 3 month old non-transgenic control, *MMTV-Wnt1* and *MMTV-ΔNβ-catenin* mice were stained with Masson's trichrome to evaluate collagen deposition. The collagen-rich area is stained blue. At least 3 mammary glands per each genotype were examined, and representative images are shown. (B) Tumor sections from *MMTV-Wnt1* and *MMTV-ΔNβ-catenin* were stained with H&E and the histological features were examined (top panel; scale bars=100 μm). To confirm the presence of activated stromal fibroblasts, tumor sections were stained with anti-α-smooth muscle actin (SMA) and K5 antibody (bottom panel). Infiltration of SMA positive fibroblast cells was evident in Wnt1-induced tumors (green, SMA; red, K5; blue, TO-PRO3; scale bars=50 μm). Representative images of stromal infiltration of Wnt1-induced tumors compared to ΔNβ-catenin-induced solid adenocarcinomas are shown. (C) The kinetics of tumor development in *MMTV-Wnt1* mice is different from that in *MMTV-ΔNβ-catenin* mice. Cohorts of virgin females from *MMTV-Wnt1* and *MMTV-ΔNβ-catenin* mice were palpated weekly to determine tumor incidence, and the tumor-free survival curve was

plotted versus time. (D) H&E stained tumors sections from Wnt1 or ΔNβ-catenin tumor cell isografts. Representative images are shown. Scale bars=100 μm.

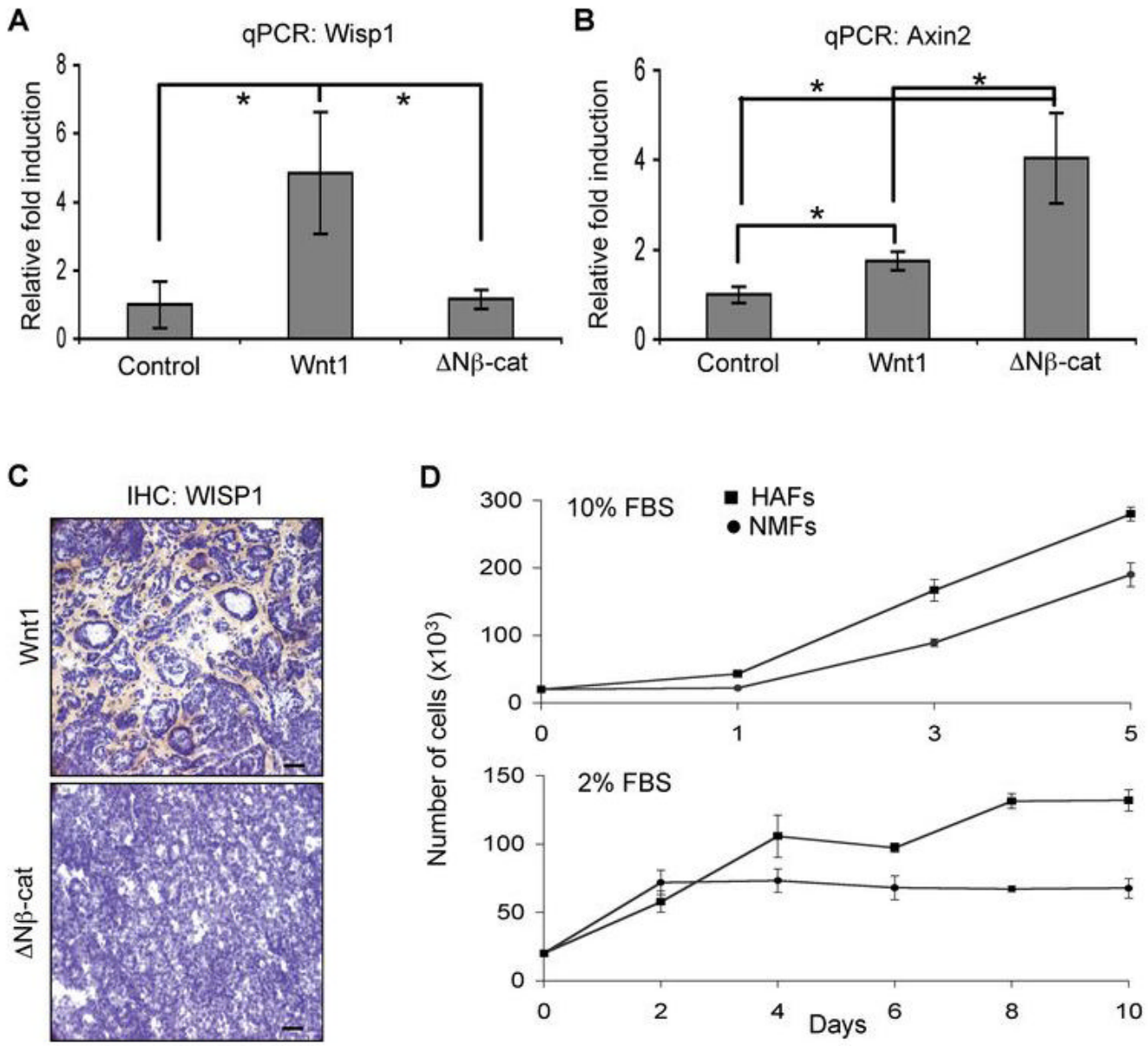

Figure 2.

Wnt1 expression in mammary epithelial cells activates surrounding stromal cells. (A) *WISP1* expression is up-regulated exclusively in Wnt1 expressing mammary glands. *WISP1* mRNA level was quantified by qPCR using total RNAs from 12~14 week old Wnt1 or ΔNβ-catenin expressing mammary glands. All data values were normalized and analyzed with the $2^{-\Delta\Delta Ct}$ method as described in Materials and Methods, and the relative fold induction was determined by dividing each sample values by control value. Bars=mean of 5 samples, error bars=standard deviation, *P<0.01. (B) A canonical Wnt signaling target gene, *Axin2* expression is induced higher levels in ΔNβ-catenin expressing mammary glands. *Axin2* mRNA level was quantified in mammary glands by qPCR to evaluate canonical signaling activity. Bars=mean of 5 samples, error bars=standard deviation, *P<0.01. (C) WISP1 is predominantly expressed by infiltrated stromal cells in Wnt1-induced tumors. Frozen sections of Wnt1- and ΔNβ-catenininduced tumors were stained with biotinylated WISP1 antibody (brown color) and

counter stained with Hematoxylin. Scale bars=100 μm. (D) The growth rate of NMFs and HAFs in either high or low serum media was measured. Error bars=standard deviation.

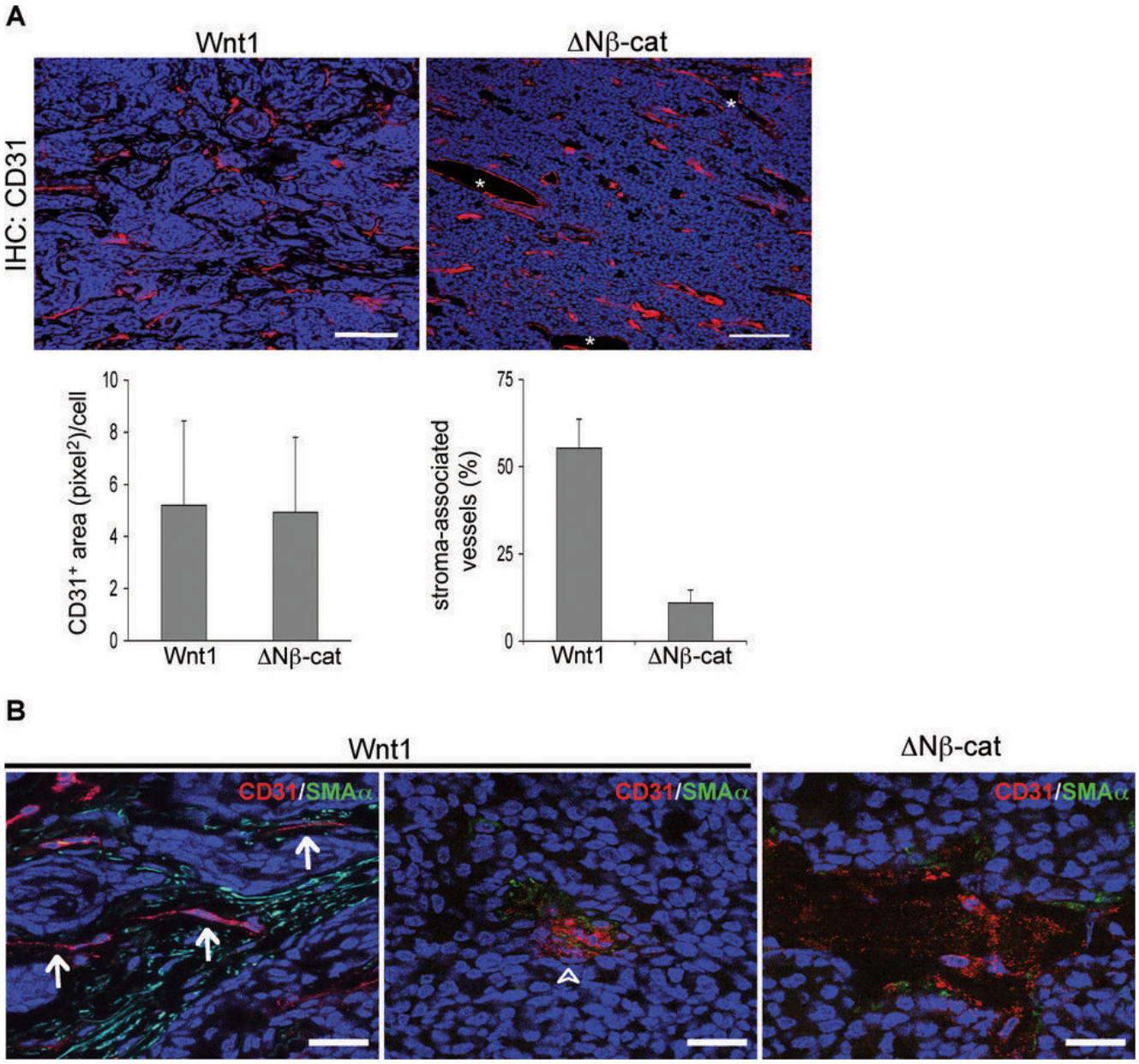

Figure 3.

Microvessel density and structure in Wnt1- and ΔNβ-catenin-induced tumors. (A) Wnt1- and ΔNβ-catenin-induced tumors have similar microvessel density. Frozen tumor sections were stained with CD31 antibody (red), and pictures were taken from at least 5 different fields per tumor (6 Group1 Wnt1-induced tumors and 5 ΔNβ-catenin-induced tumors). Note that Wnt1-induced tumors mostly have stroma-associated vessels (see Figure 3B for a higher magnification view). Vessels in ΔNβ-catenin–induced tumors were mostly mingled with tumor cells, and some dilated structures lined with $CD31^+$ cells (*) were frequently observed. Representative images are shown. Scale bars=100 μm. To determine the microvessel density (CD31 positive area per cell), the value of CD31 positive area and the number of nuclei were obtained using ImageJ software (Supplemental files; Figure 3). To quantify stroma-associated vessels, the number of stroma-associated vessels was counted and divided by total number of

blood vessels (total 30 images; 3 tumor samples per genotype). Error bars=standard deviation. (B) Stroma-associated microvessels have different structures from tumor cell-associated microvessels in Wnt1-induced tumors. To assess the microvessel structure, tumor sections were co-stained with CD31 (red color) and α-smooth muscle actin (SMA, green), and examined with higher magnification (100x objective lens). In Wnt1-induced tumors, microvessels in activated stroma area had a thin and serpentine structure (arrow), while microvessels mingled with tumor cells often had a big aggregate of endothelial cells (arrow head) that is similar to vessels in ΔNβ-catenin-induced tumors. Representative images are shown. All tissue sections were counter stained with TOPRO3 (blue color). Scale bars=20 μm.

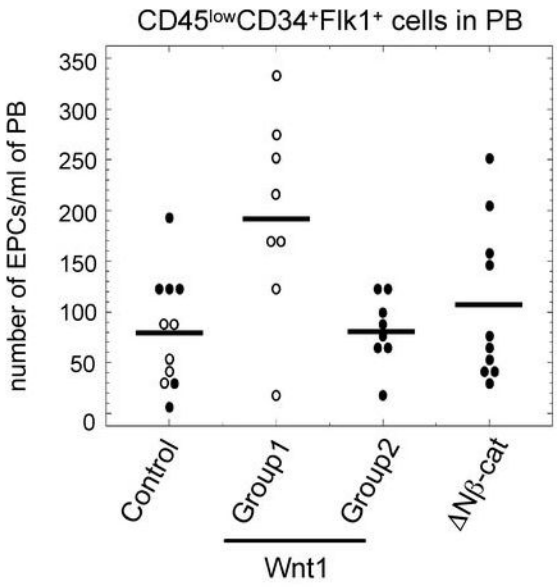

	EPCs/ml (mean±s.d)
con (n=11)	81.6 ±55.2 *
wnt1 tumor (group1; n=8)	192.8 ±96.4
wnt1 tumor (group2; n=8)	81.9 ±34.4 *
ΔNβ-cat tumor (n=10)	107.4 ±78.3 †

* P(two-sided) < 0.02, †P(two-sided)=0.062

Figure 4.

Abundant stroma correlates with higher numbers of circulating EPCs. To quantify circulating EPCs, peripheral blood (PB) cells were collected from age-matched control, Wnt1-, and ΔNβ-catenin-induced tumor bearing mice, and then analyzed with flow cytometry Cells were sorted based on marker expression ($CD45^{low}CD34^{+}Flk1^{+}$). The number of circulating EPCs per 1 ml of PB was determined as described in Materials and Methods. P value was calculated with the 2-sided Wilcoxon rank sum test. Open circle; < 120 days old, closed circle; > 120 days old.

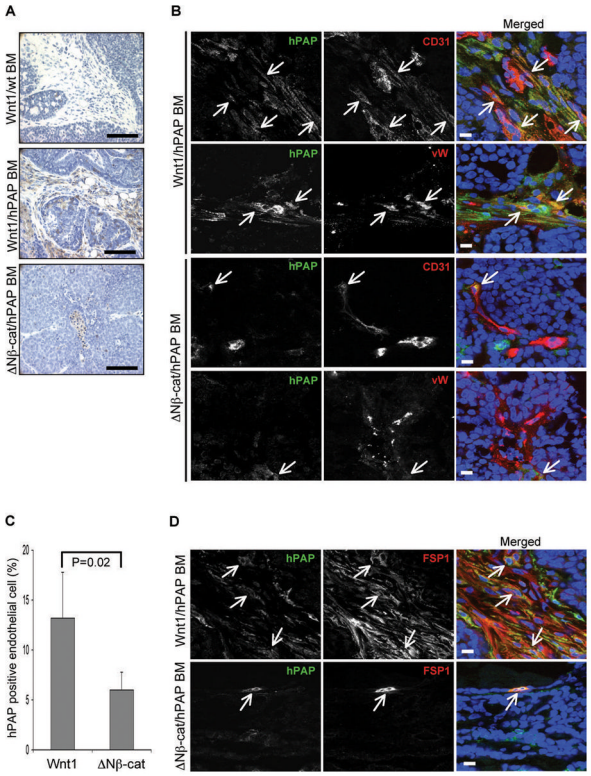

Figure 5.

BM-derived cells are recruited to Wnt1-induced tumors. (A) Immunohistochemical analysis of infiltrated BM-derived cells in Wnt1 and ΔNβ-catenin-induced tumors. Transgenic mice were lethally irradiated and transplanted with BM cells from *Rosa26-hPAP* mice. Tumor sections from those BM chimeric mice were stained with biotinylated hPAP antibody (brown color) and counter stained with hematoxylin. Wnt1-induced tumors from non-irradiated mice were used as a negative control for antibody specificity. Scale bars=100 μm (B) BM-derived cells contribute to tumor vascularization. Frozen tumor sections from BM chimeric mice were co-stained with biotinlyated hPAP antibody (green color) and either CD31 or von Willebrand factor (vW) antibody (red color), and counter stained with TO-PRO3 (blue color). A sub-population of endothelial cells was BM-derived hPAP positive cells (arrow). (C) The contribution of BM-derived cells to tumor vascularization was determined by % of hPAP and endothelial cell marker (either CD31 or vW) double-positive cells over total endothelial cells. Data were collected from total 64 images (8 different images per tumor sample and 4 tumors per genotype). Scale bars=20 μm. Error bars=standard deviation. (D) BM-derived cells contribute to tumor stromalization by differentiating into fibroblast cells. Frozen tumor sections from BM chimeric mice were co-stained with biotinylated hPAP antibody (green color) and FSP1 antibody (red color), and counter stained with TO-PRO3 (blue color). The majority of FSP1 positive cells were BM-derived hPAP positive cells (arrow). Scale bars=10 μm.

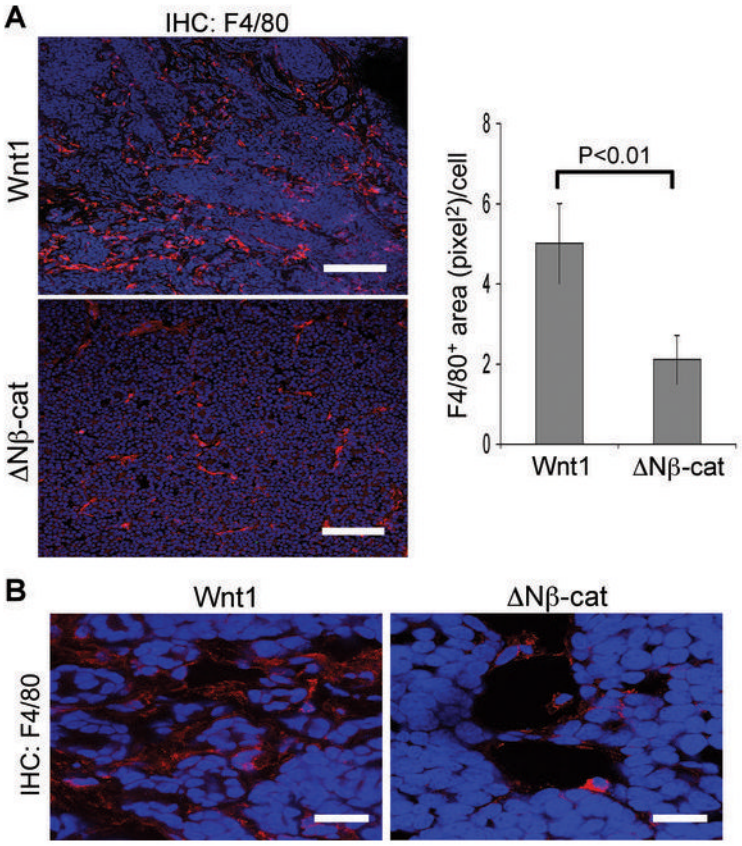

Figure 6.

More tumor-associated macrophages (TAM) are recruited to Wnt1-induced tumors. (A) Frozen tumor sections from Wnt1- and ΔNβ-catenin-induced tumors were stained with pan-macrophage marker (F4/80, red color) and counter stained with TO-PRO3 (blue color). To quantify the recruitment of TAM, the F4/80 positive area (pixel^2)/cell was determined using ImageJ software. Scale bars=100μm. Error bars=standard deviation. (B) Higher magnification images of immunohistochemistry of TAM. Scale bars=20μm.